Identification of a novel protein that regulates mitochondrial fusion by modulating mitofusin (Mfn) protein function

Yuka Eura, Naotada Ishihara, Toshihiko Oka and Katsuyoshi Mihara*

Department of Molecular Biology, Graduate School of Medical Science, Kyushu University, Fukuoka 812-8582, Japan

*Author for correspondence (e-mail: mihara@cell.med.kyushu-u.ac.jp)

Accepted 8 September 2006
Journal of Cell Science 119, 4913-4925 Published by The Company of Biologists 2006
doi:10.1242/jcs.03253

Summary

Mitofusin proteins 1 and 2 (Mfn1 and Mfn2, respectively) of the mammalian mitochondrial outer membrane are homologues of *Drosophila* FZO and yeast Fzo1, and both are essential for GTP-dependent mitochondrial fusion. We identified a 55-kDa Mfn-binding protein named MIB. It is a member of the medium-chain dehydrogenase/reductase protein superfamily, and has a conserved coenzyme-binding domain (CBD). The majority of MIB is localized in the cytoplasm but a small amount is associated with mitochondria. Exogenous expression of MIB in HeLa cells induced mitochondrial fragmentation, which was prevented by coexpression of Mfn1, suggesting a functional interaction of MIB with Mfn proteins; the GGVG sequence in the CBD of MIB is essential for its function. By contrast, MIB knockdown resulted in growth arrest of the cells, although apoptotic sensitivity was not affected by either its knockdown or its overexpression. Furthermore, MIB knockdown induced a large extension of mitochondrial network structures. By contrast, a double knockdown of MIB and Mfn1 resulted in mitochondrial fragmentation and reversal of the growth arrest, the morphology and growth phenotype induced by knockdown of Mfn1 alone, again suggesting that MIB modulates Mfn1 function. Together, these findings suggest that MIB is essential for cellular function by regulating mitochondrial membrane dynamics in cooperation with Mfn proteins.

Key words: Mitochondria, Mitochondrial fusion, Mitochondrial fission, Mitofusin proteins

Introduction

Mitochondria are extremely dynamic organelles, and they frequently change their morphology depending upon the cell environment or pathological conditions (Shaw and Nunnari, 2002; Karbowski and Youle, 2003; Chen and Chan, 2004; Okamoto and Shaw, 2005). The dynamic behavior of mitochondria is crucial for many cellular functions (Karbowski and Youle, 2003; Chan, 2006). Mitochondrial shape is maintained under a balance of mitochondrial fusion and division (Sesaki and Jensen, 1999), and GTPases of large molecular size are involved in these processes. *Drosophila* and yeast Fzo1 proteins and their mammalian homologues mitofusin proteins 1 and 2 (Mfn1 and Mfn2, respectively) are mitochondrial outer membrane proteins involved in the mitochondrial fusion reaction; they are anchored to the outer membrane through the C-terminal segment, with both an N-terminal GTPase domain and a C-terminal coiled-coil segment in the cytoplasm. Mfn1 and Mfn2 are both essential for mammalian mitochondrial fusion (Chen et al., 2003; Eura et al., 2003), and knockout of either gene is embryonic lethal (Chen et al., 2003). Cultured cells lacking either of the Mfn proteins exhibit a distinct type of fragmented mitochondria and similar results are obtained for Mfn1- or Mfn2-knockdown cells (Chen et al., 2003; Eura et al., 2003). The mammalian dynamin-related protein Drp1 (also named Dlp1) localizes mainly, like its yeast orthologue Dnm1, to the cytoplasm, partially associates with mitochondria or peroxisomes, and is involved in mitochondrial and peroxisomal fission (Shaw and Nunnari, 2002; Karbowski and Youle, 2003; Koch et al., 2003a; Chan, 2006). Upon induction of apoptosis, Drp1 colocalizes to the mitochondrial fission foci with Bax (Frank et al., 2001; Lee et al., 2004; Youle and Karbowski, 2005). Drp1K38A, the dominant-negative form of Drp1 with a mutated GTPase domain induces, when exogenously expressed, the growth of mitochondrial tubular-network structures and simultaneously inhibits the progression of apoptosis (Frank et al., 2001). In yeast, the mitochondrial outer membrane C-tail anchor-protein Fis1 functions as the receptor of cytoplasmic Dnm1 via the peripheral adaptor proteins Mdv1 and Caf4, and mediates mitochondrial fission (Shaw and Nunnari, 2002; Okamoto and Shaw, 2005). Fis1 and Dnm1 have orthologues in many other eukaryotes including humans, although Mdv1 and Caf4 have only been identified in yeast. Human Fis1 (hFis1) is a C-tail anchor protein with two TPR segments in the N-terminal cytoplasmic domain. Whether hFis1 functions as the Drp1 receptor and interacts with any peripheral adaptor proteins, such as Mdv1 and Caf4, remains to be clarified.

Yeast Mgm1 and the mammalian counterpart OPA1, are dynamin-like proteins of the mitochondrial inner membrane both of which have a C-terminal GTPase domain in the intermembrane space (Shaw and Nunnari, 2002; Olichon et al.,

Journal of Cell Science

Journal of Cell Science

2002). They are involved in both mitochondrial membrane fusion and inner-membrane remodeling (Olichon et al., 2003; Okamoto and Shaw, 2005). Mgm1 is present as a large (high molecular size) and a small (processed, small molecular size) isoform (l-Mgm1 and s-Mgm1, respectively) (Herlan et al., 2004). The processing is mediated by Pcp1 (also named Mdm37, Ugo2 or Rbd1), and the presence of both Mgm1 isoforms is essential for mitochondrial function (Herlan et al., 2003; McQuibban et al., 2003; Sesaki et al., 2003). Mammalian OPA1 is the gene product of *OPA1*, mutations of which cause the optic atrophy type I (Alexander et al., 2000; Delettre et al., 2000). Cipolat et al. (Cipolat et al., 2004) demonstrated that OPA1 requires Mfn1 to promote mitochondrial fusion.

To date, genetic or genomic approaches in yeast and mammals have identified several proteins distinct from the large molecular size GTPases described above, such as Ugo1, Mdm30 (mitochondrial distribution and morphology 30) and Mdm33 in yeast, and Dap3 (death-associated protein 3), MTP18 and endophilin B1 (also named Bif-1 or SH3GLB) in mammals. Ugo1 is a mitochondrial bi-topic outer-membrane protein involved in mitochondrial fusion (Sesaki and Jensen, 2004). Ugo1 and Fzo1 exhibit distinct localization on the outer membrane and they probably mediate distinct steps of the mitochondrial fusion reaction (Sesaki and Jensen, 2004). Mdm33 is a 54-kDa inner-membrane protein with two transmembrane domains and at least three coiled-coil structures, and is involved in inner-membrane fission (Messerschmitt et al., 2003). Mdm30 is an ~70-kDa protein localized mainly in the cytoplasm but also in mitochondria that is required for maintaining fusion-competent mitochondria (Fritz et al., 2003). It contains an F-box motif that is commonly found in the Skp1-cullin-F-box (SCF) ubiquitin ligase and modulates mitochondrial morphology through regulation of the steady-state level of Fzo1 (Fritz et al., 2003; Escobar-Henriques et al., 2006). Dap3 is a 46-kDa protein that contains a GTP-binding domain, is localized in the mitochondrial matrix and is involved in the apoptosis-induced fission process (Mukamel and Kimchi, 2004). MTP18 (mitochondrial protein 18-kDa) is an integral inner-membrane protein that is a transcriptional downstream target of PI3-kinase signaling. Its overexpression induces mitochondrial fragmentation and its knockdown induces highly fused mitochondria, suggesting that it is an essential intra-mitochondrial component of the mitochondrial division apparatus (Tondera et al., 2004; Tondera et al., 2005). Of note, knockdown of MTP18 increases apoptosis sensitivity of cells. Endophilin B1, a member of the fatty acid acyl-transferase family, has lipid-tubulating activity and can directly interact with Bax (Pierrat et al., 2001; Cuddenback et al., 2001). It cycles dynamically between the cytosol and mitochondria, and a transient mitochondrial accumulation of endophilin B1 is observed upon apoptotic induction (Karbowski et al., 2004). Knockdown of endophilin B1 disrupts coupling between the outer and inner membranes, and vesicles or tubules of the outer membrane are formed.

In the present study, we identify a novel protein, which interacts with Mfn proteins and is essential for cell growth, and which negatively regulates the dynamics of the mitochondrial membrane by modulating Mfn1 function. We named this protein mitofusin-binding protein (MIB).

Results

Identification of a 55-kDa protein as MIB

To analyze the regulatory mechanisms of mitochondrial fusion by Mfn proteins, we searched rat liver cytosol for Mfn-interacting protein(s) using a chimeric protein (MBP-Mfn1ΔC) in which maltose-binding protein (MBP) was fused to the N-terminal end of the cytosolic domain of Mfn1 (Mfn1ΔC) as the affinity matrix. Application of rat liver cytosol to the MBP-Mfn1ΔC column revealed that an approximately 55-kDa protein was specifically bound to the column and eluted with 300 and 500 mM NaCl (arrow in Fig. 1A). This protein did not bind to a control MBP-column (MBP in Fig. 1A). cDNA cloning based on the primary sequence of the peptide fragment revealed that it was a 404-amino-acid protein encoded by the MIB cDNA (accession number NP_001028855, NCBI database). This protein is a rat homologue of vesicle amine transferase 1 (VAT-1) from *Torpedo* synaptic vesicles, which bears similarity to eye lens ζ-crystallin and *E. coli* quinone oxidoreductase that all belong to the medium-chain dehydrogenase/reductase protein superfamily (Linial et al., 1989; Linial and Levius, 1993a; Persson et al., 1994). VAT-1 is firmly associated with the membrane and exhibits ATPase activity (Linial and Levius, 1993b), although its physiological function remains to be elucidated. Its calculated molecular size is 43,116 Da, although, for unknown reasons, both endogenous and recombinant forms of MIB migrated at a size lower than 55 kDa when SDS-PAGE was carried out (see Fig. 1D). The hydropathy profile revealed that there are no obvious transmembrane domains within the molecule and that it has an ~34% overall sequence identity with ζ-crystallin and 78% identity in the 14-residue coenzyme-binding domain (CBD) containing the conserved GGVG-motif (Fig. 1B,C, and see Fig. 5A). On the basis of the properties described below, we named this protein mitofusin-binding protein (MIB). When the extract prepared from HeLa cells expressing exogenous MIB-FLAG was applied to the MBP-Mfn1ΔC column, it bound to the matrix and was eluted with 300 mM or 500 mM NaCl, confirming the above findings (Fig. 1D). There was no significant binding to the control MBP-column (Fig. 1D). To further confirm the binding specificity, FLAG-tagged Mfn1 or Mfn2 was coexpressed with MIB-HA in HeLa cells and the isolated mitochondria were subjected to immunoprecipitation after digitonin solubilization, which revealed that rat MIB interacted with both Mfn1 and Mfn2 (see Fig. 6C). The interaction between MIB and Mfn proteins was not affected by the presence of GTP or ATP (data not shown). Tissue-distribution, analyzed by immunoblotting using specific antibodies raised against recombinant rat MIB, revealed that it was generally expressed in all the tissues examined (Fig. 2A).

Cell fractionation of rat liver under isotonic conditions indicated that MIB localized mainly in the cytoplasm, and partly in the membrane fractions containing the mitochondria and microsomes (Fig. 2B). Confirming these results, analysis of the post-nuclear membrane fraction (Fig. 2C, membrane) using sucrose-density-gradient centrifugation revealed that a large fraction was recovered in the supernatant and the remainder was co-sedimented with the membrane fractions containing the endoplasmic reticulum (ER) and mitochondria. MIB co-sedimented with lighter mitochondrial fractions, and exogenously expressed MIB-FLAG was not uniformly localized on the fragmented mitochondria (see Fig. 3A).

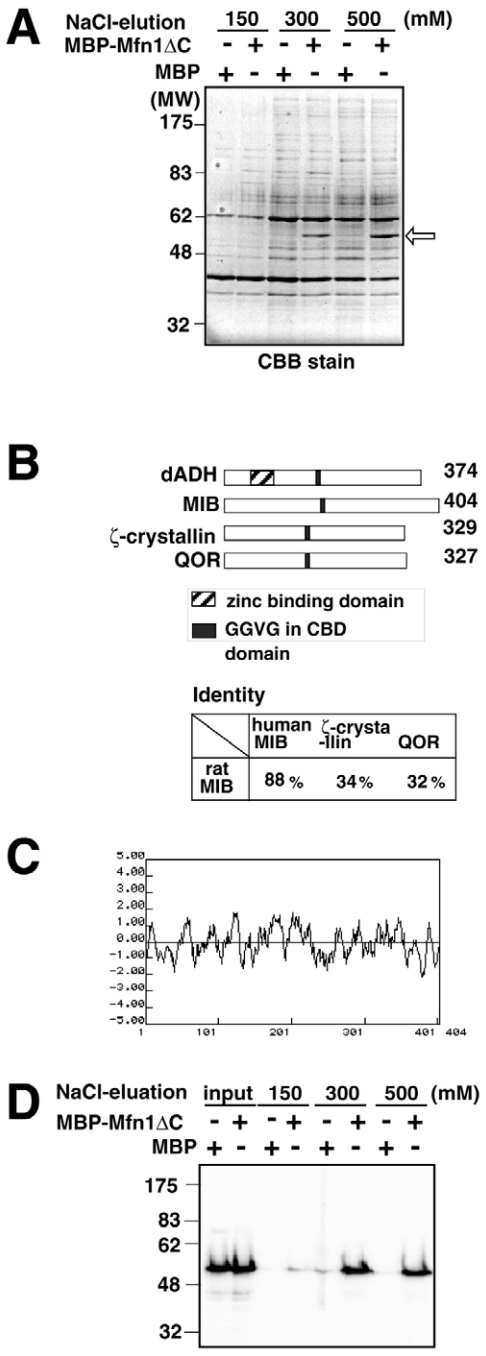

Fig. 1. Identification of the Mfn-binding protein (MIB). (A) Isolation of MIB using MBP-MfnΔC-conjugated resin from rat liver cytosol. MBP-Mfn1ΔC- or MBP-conjugated resin were treated with the indicated concentrations of NaCl. The eluted proteins were analyzed by SDS-PAGE and CBB-staining. (B) Schematic representation and sequence identity of medium-chain dehydrogenase/reductase protein superfamily. dADH, medium-chain alcohol dehydrogenase; QOR, *E. coli* quinone oxidoreductase. (C) Hydropathy profile of rat MIB deduced by Kyte and Doolittle algorithm with a 10-amino-acid-residue window. (D) Elution profile of MIB-FLAG from MBP-MfnΔC-conjugated resin. Cytosolic fraction prepared from MIB-FLAG-expressing HeLa cells was incubated with MBP-Mfn1ΔC beads, then eluted by buffer containing the indicated concentrations of NaCl as in (A). The eluted proteins were analyzed by SDS-PAGE and subsequent immunoblotting using anti-flag antibody.

However, the functional significance of this heterogenous distribution is not known. Furthermore, when the isolated mitochondria were subjected to the same sucrose-density-gradient centrifugation, a significant fraction was released from the membrane to the supernatant and the other fraction remained associated with the mitochondria (Fig. 2C, mit). MIB recovery in the mitochondria was at its maximum (~50%) in 150 mM NaCl, whereas it decreased under higher or lower salt conditions (data not shown). Thus, two populations of MIB were evident; a fraction peripherally associating with the mitochondrial membrane mainly through ionic interactions, and a fraction associating with the membrane through some other interactions, including hydrophobic interactions. The mitochondria-bound MIB was completely digested by 50 μg/ml proteinase K or extracted with sodium carbonate (pH 11.5) under isotonic conditions, indicating that it is associated with the mitochondrial surface (data not shown). Together, these findings indicate that MIB peripherally associates with the outer surface of mitochondria. A significant fraction of MIB, which

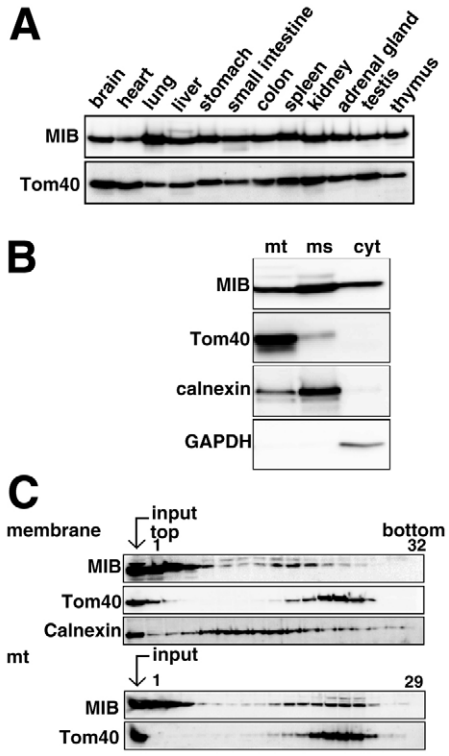

Fig. 2. Tissue expression and membrane-binding properties of MIB. (A) Rat tissues were analyzed by SDS-PAGE and subsequent immunoblotting using anti-MIB and anti-TOM40 antibodies. (B) Subcellular fractionation of rat liver MIB. Rat liver was fractionated under isotonic buffer containing 150 mM NaCl into mitochondrial (mt), microsomal (ms) and cytosolic (cyt) fractions (20 μg per well), which were analyzed by SDS-PAGE and subsequent immunoblotting using anti-MIB, TOM40 (mitochondrial marker), calnexin (ER marker), and glyceraldehyde-3-phosphate dehydrogenase (GAPDH; cytosolic marker). (C) Sucrose-density-gradient-centrifugation profiles of rat liver post-nuclear membrane fraction (membrane) and mitochondrial fraction (mt). The post nuclear fraction or isolated mitochondria was subjected to sucrose-gradient centrifugation at 77,600 ***g***, for 3 hours as described in Materials and Methods.

behaved like the mitochondria-bound form, was also recovered from the microsomal fraction, although colocalization of exogenously expressed MIB-FLAG with the ER was not obvious by fluorescence microscopy (see Fig. 3C, bottom panels). MIB specifically affected mitochondrial morphology and not the morphology of other organelles, such as ER, Golgi or peroxisomes, as evidenced by fluorescence microscopy (see below). The function of ER-associated MIB is not known.

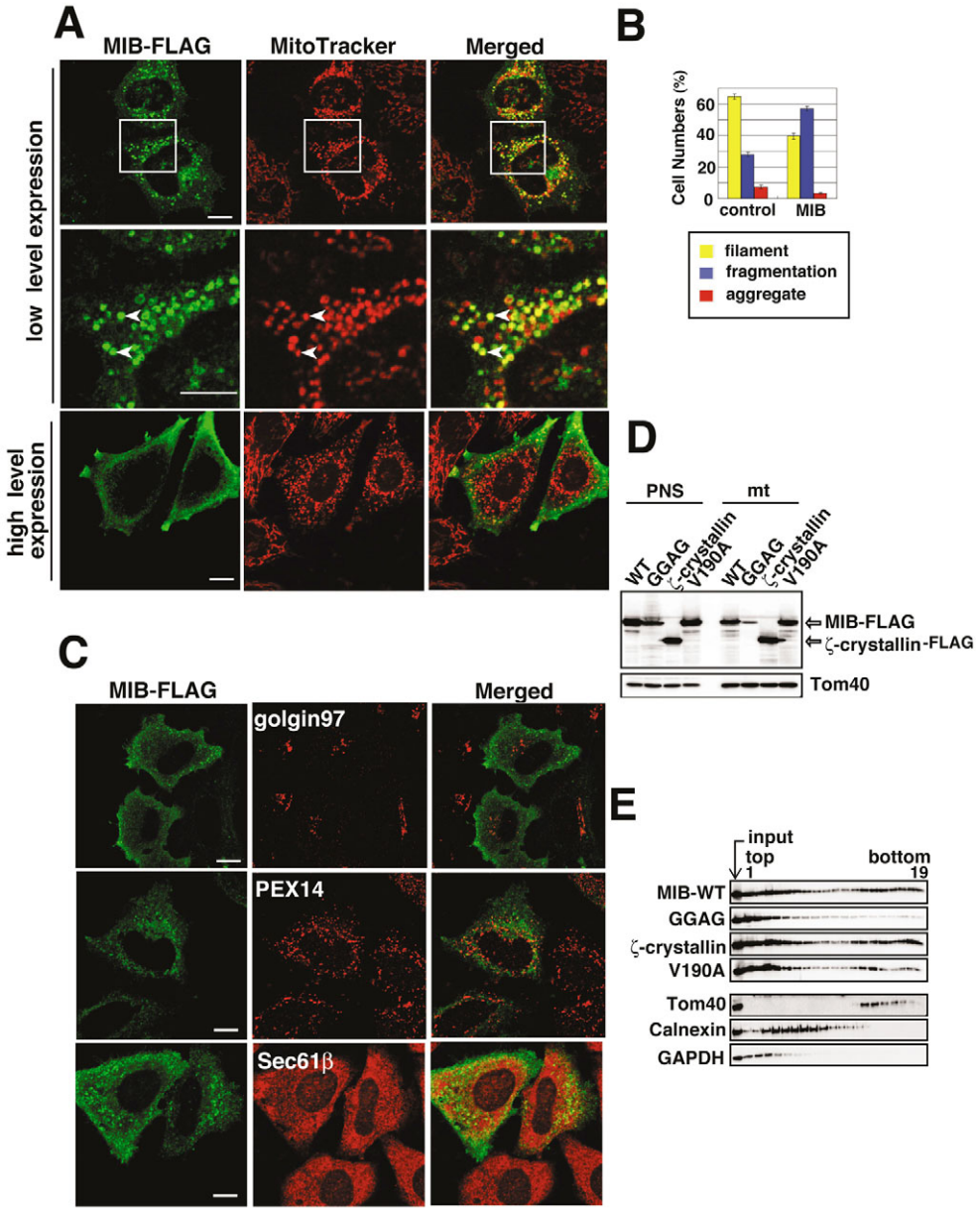

Fig. 3. Effect of exogenously expressed MIB-FLAG on mitochondrial morphology in HeLa cells. (A) Rat MIB-FLAG was expressed in HeLa cells and the cells were counter-stained with MitoTracker and analyzed by immunofluorescence microscopy using anti-flag antibody. MIB-FLAG-stained fragmented mitochondria are indicated by arrowheads. Bars, 10 μm. Details of the boxed regions in upper panels are shown in the middle panels. Images of MIB-FLAG high expressed cells are shown in the lower panels. (B) Cells with filamentous network mitochondria, fragmented mitochondria and aggregated mitochondria were counted. More than 100 cells were counted for at least three different optical fields. (C) Effect of exogenously expressed MIB-FLAG on the morphology of the ER, Golgi and peroxisomes. The MIB-FLAG expressed HeLa cells were counterstained with antibodies against Sec61β (ER marker), Golgin97 (Golgi marker), or Pex14 (peroxisome marker) as described in the Materials and Methods, and examined by fluorescence microscopy. Bars, 10 μm. (D) HeLa cells expressing the indicated constructs (FLAG-tagged) were fractionated and the postnuclear supernatant (PNS) and the mitochondrial fractions (20 μg per well) were analyzed by SDS-PAGE and subsequent immunoblotting using antibodies against flag and Tom40. (E) PNS from cells expressing the indicated constructs were subjected to sucrose-density-gradient centrifugation as described in Materials and Methods. The centrifuged solutions were fractionated and analyzed by SDS-PAGE and subsequent immunoblotting using antibodies against flag, Tom40 (mitochondria marker), calnexin (ER marker) and GAPDH (cytosolic marker).

Journal of Cell Science

Exogenous expression of MIB induces mitochondrial fragmentation

We then examined the effect of MIB on mitochondrial morphology using immunofluorescence microscopy. When C-terminally flag-tagged MIB (MIB-FLAG) was expressed in HeLa cells at low levels, it localized to the cytoplasm and was present in membrane fractions containing mitochondria (Fig. 3A, arrowheads; Fig. 3D,E), which led to extensive mitochondrial fragmentation (Fig. 3A,B). When expressed at high levels, MIB-FLAG tended to be concentrated in the periphery of the cells. Although mitochondrial fragmentation did occur, mitochondrial distribution was not affected (Fig. 3A, bottom panels; also see Fig. 4A and Fig. 8B). By contrast, no clear morphological changes were induced in the ER, Golgi or peroxisomes as detected by immunofluorescence microscopy using antibodies against Golgin97, Pex14 and Sec61β for Golgi, peroxisomes and microsomes, respectively (Fig. 3C), indicating that the effect of MIB was specific for mitochondria.

Mutations in the GGVG-motif compromise the ability of MIB to stimulate mitochondrial fragmentation

To investigate whether the GGVG-motif in the CBD of MIB has an important role in stimulating mitochondrial fragmentation, we used mutants in which one or two amino acid residues of the motif were substituted with alanine. In contrast to wild-type MIB, all of the mutants failed to induce mitochondrial fragmentation (Fig. 4A,B), although they were expressed at similar levels (Fig. 4C). Interestingly, the mitochondrial targeting was compromised by these mutations (Fig. 3D,E for GGAG mutant; data not shown for the other mutants). As a negative control, alanine substitution within arbitrarily selected tetra-peptide regions (containing a VG pair) outside the CBD (V13A and V190A in Fig. 4A) did not affect MIB stimulation of mitochondrial fragmentation, and mutants were efficiently targeted to the mitochondria (V190A in Fig. 3D,E; V13A, not shown). Confirming these results, the MIB construct carrying a mutation in the GGVG-motif failed to bind to MBP-Mfn1(ΔC) (Fig. 4D, GGAG). We thus concluded that

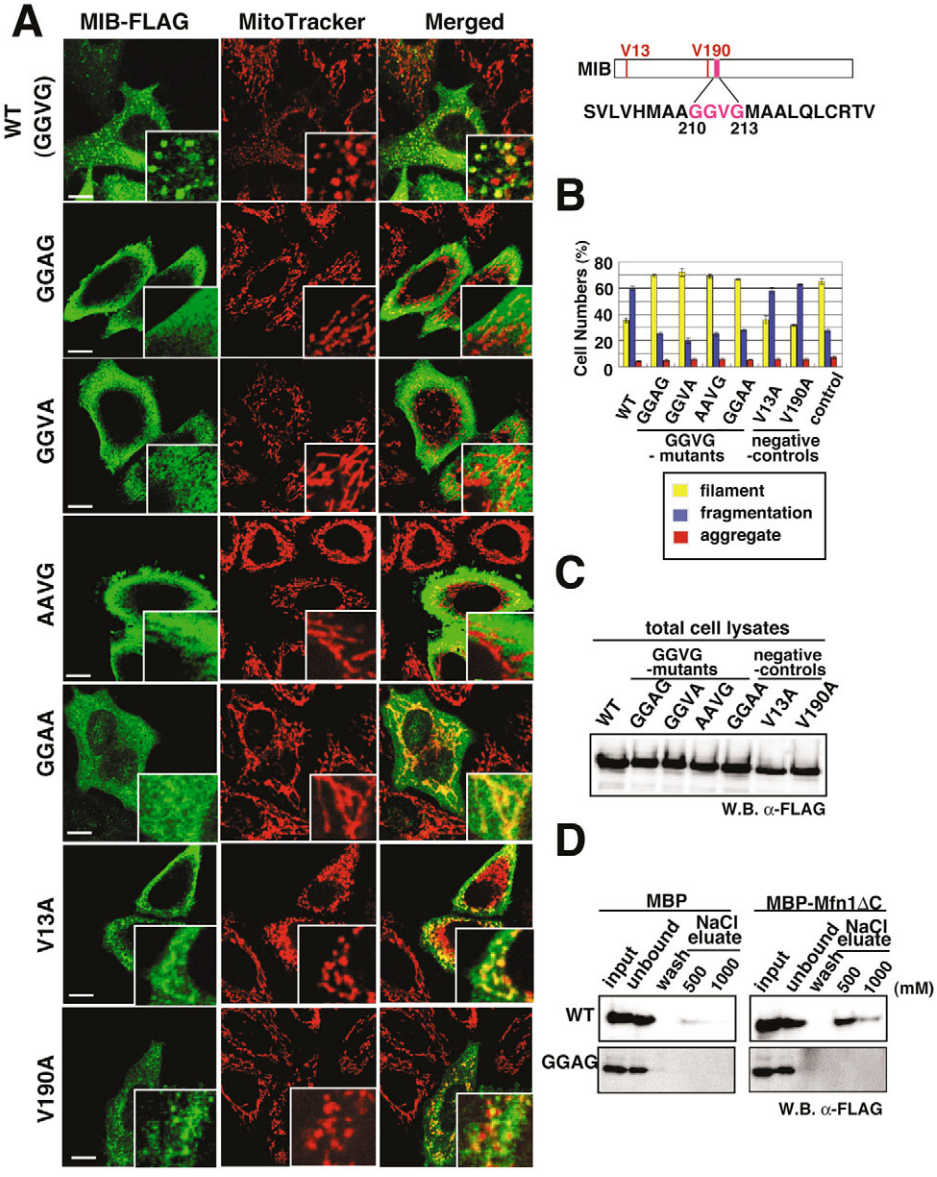

Fig. 4. Effect of MIB-FLAG constructs carrying mutation in the GGVG-motif on mitochondrial morphology. (A) MIB-FLAG proteins with the indicated mutations in the GGVG-motif were expressed in HeLa cells and examined by fluorescence microscopy as in Fig. 3. The constructs V13A and V190A carrying a mutation in the arbitrarily selected tetrapeptide region (containing GV) outside the GGVG-motif were examined as the negative controls. Bars, 10 μm. (B) Cells with the indicated mitochondrial morphology shown in A were quantified. More than 100 cells were counted in at least three distinct optical fields. Control: empty vector. (C) Expression levels of the indicated constructs were analyzed by SDS-PAGE and subsequent immunoblotting using anti-flag IgG. (D) Wild-type MIB-FLAG or the GGAG-mutant were exogenously expressed in HeLa cells, and the cytosolic fractions incubated with MBP- or MBP-Mfn1ΔC-conjugated beads. Proteins bound to the beads were eluted by buffer containing the indicated concentrations of NaCl, and eluted proteins were analyzed by SDS-PAGE and subsequent immunoblotting with anti-flag antibodies.

the conserved CBD of MIB is essential for both Mfn binding and induction of mitochondrial fragmentation.

As described above, ζ-crystallin and MIB exhibit an overall sequence identity of 34%. In their sequences, the 14-amino-acid region containing the GGVG-motif in the CBD is highly conserved (78%; Fig. 1B and Fig. 5A). We therefore examined the effect of exogenous expression of flag-tagged ζ-crystallin (ζ-crystallin-FLAG) on mitochondrial morphology. It was expressed to a similar extent as MIB (Fig. 5C) and a significant fraction was targeted to the mitochondria (see Fig. 3D,E). Mitochondrial morphology, however, was not affected by the expression (Fig. 5B,D). Confirming these results, HeLa cell-ζ-crystallin-FLAG, in contrast to wild-type MIB, failed to bind to MBP-Mfn1(ΔC) (Fig. 5E). Together, these results indicate that the CBD-containing segment and the sequence unique to MIB were both required for MIB to bind Mfn1 and to induce mitochondrial fragmentation.

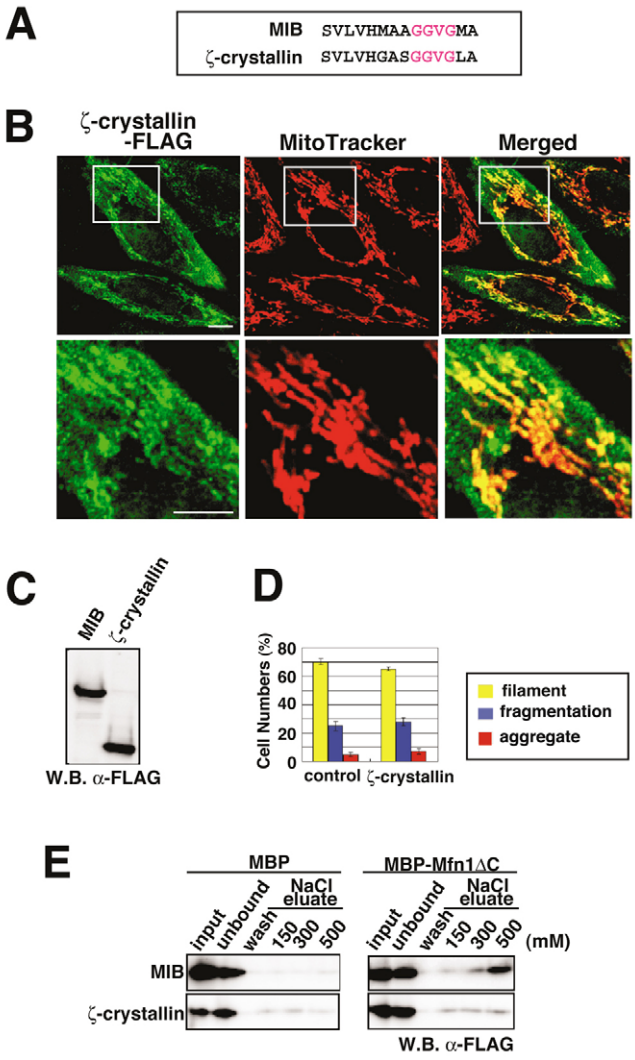

Fig. 5. Exogenously expressed ζ-crystallin does not affect mitochondrial morphology, although it is targeted to the mitochondria. (A) Comparison of amino acid sequences of the GGVG-motif-containing regions of MIB and ζ-crystallin. (B) Mitochondrial morphology of HeLa cells expressing ζ-crystallin-FLAG. Intracellular localization of ζ-crystallin was analyzed by immunofluorescence microscopy. Mitochondria were counterstained with MitoTracker. Details of the boxed regions in top panels are shown in the bottom panels. Bars, 10 μm. (C) Expression levels of MIB-FLAG and ζ-crystallin-FLAG in HeLa cells were examined by SDS-PAGE and subsequent immunoblotting with anti-FLAG IgG. (D) Cells with the indicated mitochondrial morphology shown in B were quantified. At least 100 cells were counted in at least three distinct optical fields. Control: empty vector. (E) Binding of ζ-crystallin-FLAG to Mfn1 as examined by MBP-Mfn1ΔC-beads. HeLa cell extracts expressing ζ-crystallin-FLAG or MIB-FLAG were incubated with MBP- or MBP-Mfn1ΔC-conjugated beads. Other conditions were as described in Fig. 1D.

Mitochondrial fragmentation-stimulating activity of MIB is offset by the coexpression of Mfn proteins

Since MIB was identified as a protein having Mfn1 affinity, we analyzed whether the action of MIB on mitochondrial morphology described above was affected by coexpression of Mfn proteins in vivo. As demonstrated previously, exogenously expressed Mfn1-HA in HeLa cells was targeted to mitochondria, and induced aggregation of mitochondria together with an extension of outer membrane tubular structures emanating from the aggregated mitochondria (Eura et al., 2003) (see Mfn1-HA in Fig. 6A). When Mfn1-HA was coexpressed with MIB-FLAG, however, the fragmented mitochondria were significantly diminished and, in turn, mitochondria with network structures were increased (Fig. 6A,B). In this context, we examined whether exogenously expressed Mfn proteins and MIB in HeLa cells physically interact with each other. When mitochondria harboring both Mfn-FLAG and MIB-HA were solubilized by digitonin and subjected to immunoprecipitation with anti-HA-IgG, Mfn1-FLAG and Mfn2-FLAG coprecipitated with MIB-HA in a GTP-independent manner (Fig. 6C). As a control, the Mfn-FLAG signal was not detectable in the absence of the antibody. It should be noticed that morphological detection of the interaction between MIB and Mfn2 was difficult because Mfn2-overexpression did not exhibit a typical synchronous mitochondrial phenotype (Eura et al., 2003).

Knockdown of MIB induces extensive growth of mitochondrial network structures

We then examined the effect of MIB-knockdown on mitochondrial morphology. Immunoblotting revealed that exogenously expressed MIB was depleted by ~75% (Fig. 7A). Quantitative PCR indicated that the endogenous MIB was also depleted by ~95% (data not shown). This manipulation produced mitochondria with extensive network structures (Fig. 7B,C). In addition, the MIB-depleted cells expanded frequently and were sometimes polykaryonic (Fig. 7B,H) as if cytokinesis was compromised. When the outer and inner membranes were co-immunostained with antibodies against Tom20 and mitofilin for the outer and inner membranes, respectively, tubular structures or distinctly stained tubular structures were frequently observed, which were seldom observed in control RNA interference (RNAi) cells (Fig. 7D). Similar structures were observed in the cells double-stained with antibodies against Tom20 and MitoTracker. As a control, Fis1-RNAi and Mfn1-RNAi did not produce such phenotypes (data not shown). The morphology of the other organelles such as ER, Golgi and peroxisomes was not affected by the MIB-knockdown (Fig. 7E), again indicating that MIB is specifically

Journal of Cell Science

Journal of Cell Science

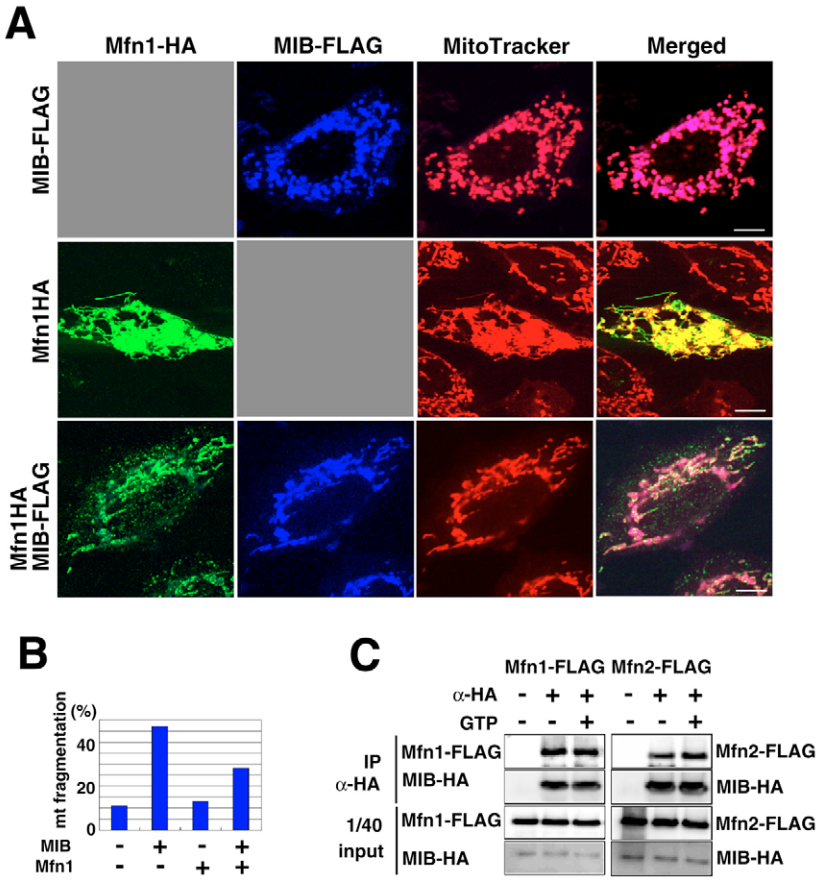

Fig. 6. Mitochondrial fragmentation-stimulating activity of MIB is offset by the coexpression of Mfn proteins. (A) Mfn1-HA, MIB-FLAG, or both were transfected to HeLa cells and the mitochondrial structures of the cells were examined by immunofluorescence microscopy as described in Materials and Methods. Bars, 10 μm. (B) The cells containing fragmented mitochondria were quantified. At least 100 cells were counted in three distinct optical fields. (C) Mfn1-FLAG or Mfn2-FLAG (Eura et al., 2003) was coexpressed with MIB-HA in HeLa cells. The mitochondria were isolated from the cells and solubilized by 1% digitonin. The solubilized fractions were subjected to immunoprecipitation using anti-HA IgG under the indicated conditions. The immunoprecipitates were analyzed by SDS-PAGE and subsequent immunoblotting with anti-HA or anti-FLAG IgGs.

involved in mitochondrial morphological changes. Tom20-positive, but mitofilin- or MitoTracker-negative tubular structures were frequently observed in the periphery of the extended mitochondrial network structure, as if the inner and outer membranes were dissociated in this area.

MIB knockdown leads to growth inhibition of the cells without affecting apoptosis-sensitivity.

MIB knockdown induced expansion of cells and, at the same time, cell growth was significantly arrested (Fig. 7F,G). Importantly, this growth delay was offset by additional depletion of Mfn1, concomitant with mitochondrial morphological changes from extended network to fragmented structures, a Mfn1-knockdown phenotype (Fig. 7G and Fig. 8D). These results clearly indicated that the MIB-Mfn1-dependent regulation of mitochondrial dynamics is essential for cellular functions.

It is generally believed that mitochondrial morphology is intimately related to apoptosis (Karbowski and Youle, 2003; Youle and Karbowski, 2005). Cells with extended mitochondria are resistant to apoptosis, whereas cells with fragmented mitochondria are sensitive to apoptotic signals. We therefore analyzed the sensitivity to apoptotic stimuli of MIB-knockdown- or MIB-overexpressing cells. As described above, MIB overexpression induced mitochondrial fragmentation, but the cells exhibited apoptosis sensitivity at levels comparable with mock-transfected cells, as assessed by cytochrome *c* release (Fig. 7I). By contrast, exogenous expression of Fis1 induced extensive mitochondrial fragmentation and, at the same time, clearly increased apoptosis-sensitivity of the cells (Fig. 7I), confirming previous reports (James et al., 2003; Lee et al., 2004). Furthermore, we analyzed whether overexpression or knockdown of MIB induces apoptosis in the cells, using poly(ADP-ribose)polymerase (PARP)-processing as a measure. There was no significant apoptosis induced compared with actinomycin-D-treated cells in either manipulation of the cells (Fig. 7J). Taken together, exogenous expression or knockdown of MIB neither induced significant apoptosis nor affected apoptosis-sensitivity of the cells.

MIB affects Mfn function to modulate the balance of mitochondrial fission and fusion

Since mitochondrial morphology is balanced by membrane fusion and fission (Sesaki and Jensen, 1999), we then addressed whether MIB affects mitochondrial fission or mitochondrial fusion directly. In yeast, the Dnm1-Fis1 system cooperating with the peripheral adaptor proteins Mdv1 or Caf4 is the sole mitochondrial division machinery. Moreover, exogenous expression of Fis1 in mammalian cells induces extensive mitochondrial fragmentation and, conversely, depletion of Fis1 induces extension of the mitochondrial networks, although the evidence that Fis1 functions as a membrane receptor for Drp1 via some peripheral adaptor protein(s) is missing. As expected from the above results, the extended mitochondrial network structures formed by Fis1-depletion (~95%; Fig. 8A) was clearly attenuated by MIB expression to result in an MIB-overexpression phenotype and, vice versa, mitochondrial

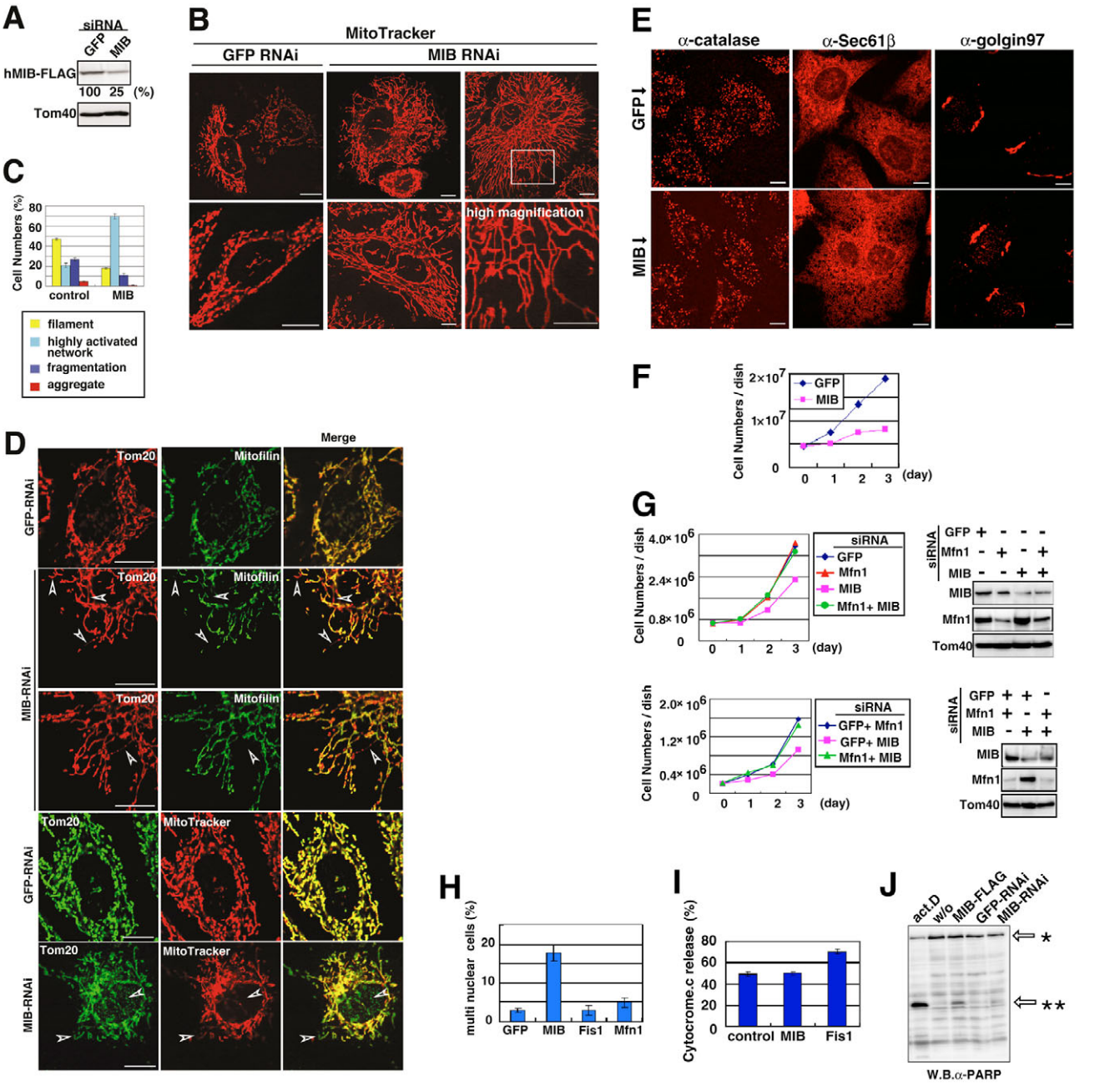

Fig. 7. Knockdown of MIB induced extensive growth of mitochondrial network structures. (A) HeLa cells were transfected with MIB siRNA or, as a control, with GFP siRNA as described in Materials and Methods. The cell extracts (20 μg per well) were subjected to SDS-PAGE and subsequent immunoblotting using anti-flag or anti-Tom40 IgGs. (B) The MIB-RNAi cells and GFP-RNAi (control) cells were stained with MitoTracker and examined for mitochondrial morphology by fluorescence microscopy. Bars, 10 μm. (C) Quantification of cells with the indicated mitochondrial morphology. At least 100 cells were counted in three distinct optical fields. (D) RNAi cells for the indicated proteins were analyzed by immunofluorescence microscopy using the indicated antibodies or MitoTracker staining. Bars, 10 μm. (E) MIB knockdown did not affect morphology of peroxisomes, ER or Golgi complex. GFP-RNAi cells (control) or MIB-RNAi cells were analyzed by immunofluorescence microscopy using the indicated antibodies. Bars, 10 μm. (F) HeLa cells were split into eight dishes (6-cm dishes) and grown for 24 hours. Cells of one aliquot were counted after trypsin treatment using the Coulter counter (day 0). Cells in one aliquot were transfected with MIB RNAi or GFP RNAi (for a single transfection). The other aliquots were separately subjected to sequential siRNA-transfection (double or triple transfection) for MIB or GFP. Cells were all grown for 24 hours and then counted as described above. (G) HeLa cells were transfected with the indicated combinations of siRNAs according to the protocol as described in F, except that 3.5-cm dishes were used. (H) Polykaryonic cells were analyzed for cells transfected with the indicated plasmids. At least 100 cells were counted in three distinct optical fields. (I) HeLa cells exogenously expressing the indicated proteins were grown for 24 hours. The cells were cultured in the presence of 20 μM actinomycin D and 100 μM zVAD-fmk for 7 hours, which were then analyzed by immunofluorescence microscopy using anti-cytochrome *c* and anti-flag antibodies. (J) HeLa cells were subjected to the indicated treatments and the extract (20 μg per well) was analyzed by PARP-cleavage as a measure of apoptosis. *, full-length PARP; **, PARP fragment.

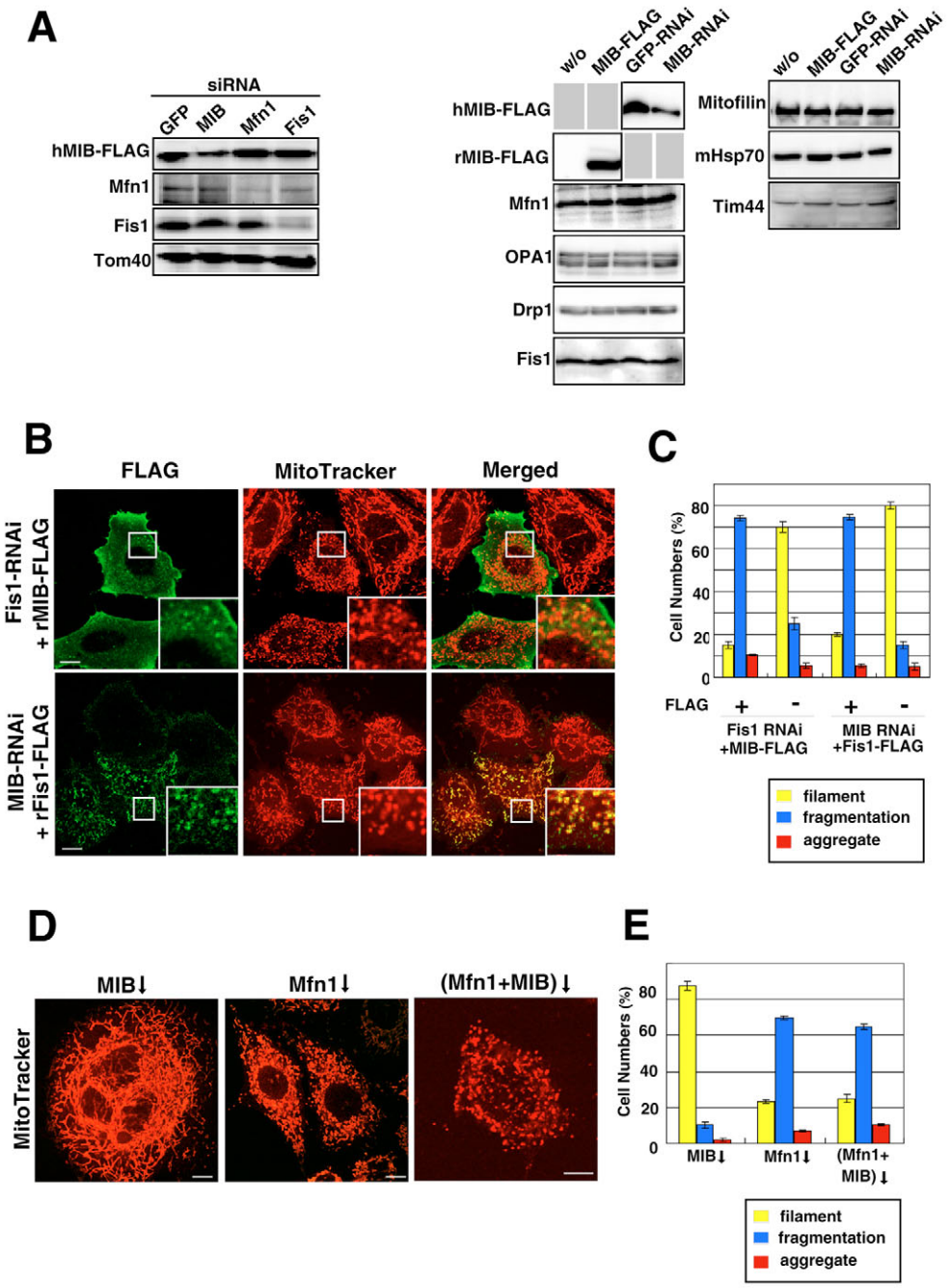

Fig. 8. MIB affects the balance of mitochondrial fusion and fission by attenuating Mfn-dependent fusion. (A) Expression levels of the components that are involved in mitochondrial morphology or mitochondrial import in HeLa cells subjected to overexpression or knockdown of MIB, Mfn1 or Fis1. HeLa cells that were subjected to the indicated manipulations (20 μg per well) were analyzed by immunoblotting using the indicated antibodies. Left panel, siRNA-treated cells. Right panels, MIB-overexpressed or siRNA-treated cells; w/o, untreated cells. (B) HeLa cells subjected to the indicated manipulations were counterstained with MitoTracker and then the flag-tag signal was analyzed by immunofluorescence microscopy. Enlarged images are boxed. Bars, 10 μm. (C) HeLa cells with the indicated mitochondrial morphology shown in B were quantified. For each experiment, at least 100 cells were counted in three distinct fields. (D) The MIB-knockdown-induced mitochondrial morphology was attenuated by Mfn1-knockdown. HeLa cells were subjected to RNAi for MIB, Mfn1 or both proteins, and examined by fluorescence microscopy after MitoTracker staining. Bars, 10 μm. (E) HeLa cells with the indicated mitochondrial morphology shown in B were quantified. For each experiment, at least 100 cells were counted in three distinct fields.

network growth by MIB-knockdown was clearly attenuated by Fis1-FLAG expression (Fig. 8B,C; compare mitochondria of MIB-FLAG-expressed with MIB-FLAG-unexpressed cells), suggesting that MIB affected mitochondrial morphology by modulating the Mfn-dependent mitochondrial fusion reaction, rather than modulating the division reaction. We further confirmed this by MIB and Mfn1 double-knockdown experiments. Knockdown of MIB induced formation of the mitochondrial network, whereas knockdown of both MIB and Mfn1 clearly inhibited network formation and induced the Mfn1-depleted phenotype (Fig. 8D,E), clearly indicating that MIB functions as a negative regulator in Mfn1-dependent mitochondrial fusion. It should be noticed that, depletion or overexpression of MIB did not affect endogenous levels of the components tested that are related to mitochondrial protein import and mitochondrial morphology regulation (Fig. 8A).

Discussion

We identified an approximately 55-kDa protein that interacts with Mfn proteins as the rat homologue of *Torpedo* VAT-1, and named it MIB. VAT-1 is a major component of *Torpedo* synaptic vesicles (Linial et al., 1989), whose homologues are detected in human epithelial cells and epithelial tissues (Hayess et al., 1998). It is a member of the medium-chain dehydrogenase/reductase protein superfamily, which includes ζ-crystallin and NADPH-quinone reductase. Their function, as well as intracellular localization, remains enigmatic, except that they exhibit ATPase activity; even the activity of vesicle

Journal of Cell Science

amine transport has not been demonstrated experimentally (see NCBI database, annotation for NP_001028855). The exogenous expression of MIB in cultured cells induced extensive fragmentation of mitochondrial networks (Fig. 3A,B). Knockdown of MIB induced the extension of mitochondrial network structures, where the MitoTracker-negative outer membrane was observed on the leading edge area of the network structures separated from the MitoTracker-positive or mitofilin-positive inner membrane (Fig. 7A-D). At the same time polykaryonic and significantly extended cells were formed (Fig. 7B,H). Furthermore, cell growth was significantly compromised by this manipulation (Fig. 7F). Interestingly, this effect was offset by simultaneous depletion of Mfn1 (Fig. 7G) – mitochondrial morphology changed from an extended network to fragmented structures – an Mfn1-knockdown phenotype (Fig. 8D). No morphological changes, however, were induced in other organelles such as ER, Golgi and peroxisomes (Fig. 7E). Endogenous levels of known components involved in mitochondrial morphological regulation as well as mitochondrial pre-protein import were not affected by these manipulations (Fig. 8A). Thus, these results suggest that MIB is essential for cell growth through regulating Mfn1-dependent mitochondrial dynamics. To our knowledge, the proteins that bring about such unique morphological changes to mitochondria by affecting the fusion reaction have not been reported.

MIB is a member of the medium-chain dehydrogenase/reductase protein superfamily, which includes ζ-crystallin, with a conserved GGVG-motif within the CBD. Unexpectedly, although a significant fraction of ζ-crystallin was targeted to the mitochondria, it neither bound to Mfn proteins nor induced mitochondrial fragmentation, which served as a suitable control for the MIB function. Furthermore, mutations introduced in the GGVG-motif of the CBD of MIB but not in other regions, compromised the activity of MIB to bind to Mfn1 and to induce mitochondrial fragmentation, thus indicating that the GGVG-motif containing segment and the other regions unique to MIB are both required for its function.

How does MIB regulate Mfn1 function? We have shown in a previous paper that Mfn1 is involved in a GTP-hydrolysis-dependent mitochondrial docking step (Ishihara et al., 2005). Considering that coenzyme NADPH contains the pseudo-nucleotide region, the CBD of MIB might recognize Mfn-bound GTP to suppress Mfn GTPase to avoid uncontrolled mitochondrial fusion reaction. Mfn proteins contain two coiled-coil regions at the N-terminal- and C-terminal-flanking sites of the bi-partite transmembrane segment, and the C-terminal coiled-coil domain is involved in mitochondrial tethering through anti-parallel dimer formation (Koshiba et al., 2004). Here, we used a Mfn1 construct lacking the C-terminal coiled-coil domain to analyze interaction with MIB constructs. Therefore, the C-terminal coiled-coil required for mitochondrial tethering did not seem to be involved in MIB interaction. The effect of MIB on Mfn GTPase activity and the region(s) of Mfn proteins required for MIB-binding remain to be analyzed. Another possibility might be that the reported activities of VAT-1 protein, i.e. ATPase activity (Hayess et al., 1998) and Ca^{2+}-dependent oligomeric-complex-forming activity (Linial, 1993; Koch et al., 2003b), regulate Mfn activity.

Mitochondrial morphology is maintained by a balance of fusion and fission. Which process is affected by MIB? Mitochondrial fusion through the inhibition of Mfn1 or mitochondrial division through stimulation of the Drp1-Fis1 system? The mitochondrial fragmentation-stimulation effect of MIB was clearly attenuated by coexpression with Mfn1 (Fig. 6A,B), and the mitochondrial network structures produced by Fis1 knockdown (~95%) were fragmented by the exogenous expression of MIB. Conversely, the network structures produced by MIB knockdown (~93%) were fragmented by overexpression of Fis1-FLAG (Fig. 8B,C). Furthermore, the network structures formed by MIB knockdown were abolished by the additional knockdown of Mfn1, and fragmented mitochondria were newly formed with the same phenotype that had been produced by a single Mfn1 knockdown, suggesting that Mfn1 limits the MIB reaction (Fig. 8D,E). These results, together with the fact that MIB was isolated by affinity for Mfn1 suggest that, MIB interacts with Mfn1 to attenuate its function. In mammals, two Mfn proteins, Mfn1 and Mfn2, are both required for mitochondrial fusion and mediate a distinct step of the fusion process (Eura et al., 2003; Ishihara et al., 2005). The issue of whether MIB affects Mfn2 activity, however, is not clear, because assessment of the functional interaction between MIB and Mfn2 based on morphological interference is difficult: Mfn2 overexpression induces a heterogenous mitochondrial phenotype, whereas overexpression of MIB induces mitochondrial fragmentation. We speculate, however, that MIB also modulates Mfn2 function in some way, because both co-precipitated in an immunoprecipitation study (Fig. 6C). The mechanism of action of both Mfn proteins in the sub-step of mitochondrial fusion must be clearly defined to understand the function of MIB.

Yeast Mdm30 is mainly localized in the cytoplasm and partially in the mitochondria (Fritz et al., 2003; Escobar-Henriques et al., 2006). Mdm30 is an SCF ubiquitin ligase and modulates mitochondrial morphology by regulating the stability of Fzo1 protein. Deletion of the gene encoding Mdm30 induces mitochondrial fragmentation. Thus, Mdm30 and MIB similarly regulate mitochondrial morphology by indirectly modulating the function or stability of Fzo1/Mfn proteins. In contrast to Δ*mdm30* cells, however, the level of mitochondrial components regulating mitochondrial morphology and protein import were unaffected in MIB-depleted or MIB-overexpressing cells (Fig. 8A).

Torpedo VAT-1 is exclusively localized to the membrane fractions containing synaptic vesicles, although the membrane-binding properties are not known. By marked contrast, cell fractionation under physiological salt conditions revealed that, a small fraction of MIB was localized in membrane fractions containing mitochondria and ER, and a vast majority was localized in the cytoplasm. The membrane-bound fraction was gradually released by incubation of the membrane in a physiological salt concentration, and efficient release was observed under low- or high-salt conditions, although a significant population remained in the membrane (data not shown). These results suggested that both ionic and other interactions, including hydrophobic interactions, are involved in membrane binding. It should be noticed that, knockdown or exogenous expression of Mfn1 did not affect the recovery of MIB in the mitochondrial fraction, suggesting that some additional factors, including Mfn2 or phospholipids, are involved in the binding.

Journal of Cell Science

How is mitochondrial targeting of cytoplasmic MIB regulated? Endophilin B1, an endophilin-I-family protein that mediates changes of the membrane curvature by lysophosphatidic acid-acyltransferase activity, is required for the regulation of mitochondrial outer membrane dynamics (Karbowski et al., 2004). The majority of endophilin B1 localizes in the cytoplasm and only a small amount is present in the mitochondria. Interestingly, its mitochondrial association is elicited by treatment of the cells with apoptotic inducers (Karbowski et al., 2004), indicating a regulated targeting of endophilin B1 to the mitochondria. Endophilin B1 seems to dynamically cycle between the cytoplasm and mitochondria in healthy cells (Karbowski et al., 2004). At present, we do not know whether MIB is a mobile factor, like endophilin B1, recycling between the cytoplasm and mitochondria. We examined whether the induction of apoptosis by pro-apoptosis reagents leads to mitochondrial targeting of MIB. In contrast to endophilin B1, no significant mitochondrial translocation of exogenously expressed MIB-FLAG was detected by fluorescence microscopy after treatment with actinomycin D (data not shown).

Recent studies suggest that mitochondrial fusion and fission processes are intimately related to apoptosis (Karbowski and Youle, 2003; Youle and Karbowski, 2005). Cells with developed mitochondrial network structures are resistant to apoptosis, whereas those with fragmented mitochondria are sensitive to apoptosis. Mitochondrial fission is induced by a variety of apoptotic stimuli such as staurosporine, recombinant Bax and recombinant p20, which result in the translocation of Drp1, Bax and endophilin B1 to mitochondrial foci, and the induction of mitochondrial fission. By contrast, dominant-negative Drp1-K38A induces the growth of network structures and counteracts the induction of apoptosis. In addition, overexpression of the fission protein Fis1 results in mitochondrial fission and cytochrome *c* release. Because exogenous expression of MIB induced extensive mitochondrial fragmentation, we analyzed cell susceptibility to apoptosis by using the release of cytochrome *c* from mitochondria as a marker. Unexpectedly, however, cells with fragmented mitochondria (due to MIB-overexpression) and mock-transfected control cells exhibited similar sensitivity to actinomycin-D-induced apoptosis (Fig. 7I). By contrast, cells with fragmented mitochondria (due to Fis1-overexpression) were sensitive to the apoptosis induction (Fig. 7I). Furthermore, there was no significant apoptosis in MIB-knockdown or MIB-overexpressing HeLa cells as examined by PARP cleavage (Fig. 7J). These data suggest that, the mitochondrial fragmentation process does not necessary cause apoptosis and probably reflects the possible function of MIB; it interferes with the Mfn1-dependent fusion reaction but does not affect the Drp1-Fis1-dependent division reaction, which might affect apoptotic sensitivity.

Materials and Methods

Materials

The rabbit polyclonal antibodies against rat Mfn1 (Eura et al., 2003), rat Fis1 (Jofuku et al., 2005), rat Tom40 (Suzuki et al., 2000), rat Tim44 (Ishihara and Mihara, 1998), and rat OPA1 (Ishihara et al., 2006) were described previously. Antibodies against human mitofilin were raised in rabbits by injecting recombinant human mitofilin (our unpublished data). The rabbit polyclonal antibodies against Pex14 and catalase were provided by Yukio Fujiki (Kyushu University, Fukuoka, Japan) and those against golgin97 were a gift from Nobuhiro Nakamura (Kanazawa University, Kanazawa, Japan). The rabbit polyclonal antibodies against hemagglutinin (HA) (Covance), Sec61β (Upstate) and calnexin (Stressgen), and the monoclonal antibodies against HA (16B12; BAbCO), flag tag (M2; Sigma), GAPDH (Ambion), mtHsp70 (ABR), Drp1 (BD bioscience), PARP (Promega), and Tom20 (Santa Cruz Biotechnology) were purchased from the indicated companies.

Affinity purification of Mfn1 interacting proteins using MBP-Mfn1ΔC column

The *Bam*HI-*Hin*dIII Mfn1ΔC fragment was excised from pET28a-Mfn1ΔC (Eura et al., 2003). The obtained fragment was subcloned into the pMALc2x vector to create the plasmid harboring MBP-Mfn1ΔC cDNA. XL1 blue cells harboring the plasmids were cultured at 37°C in 0.3 mM IPTG for 3 hours. The N-terminal MBP-tagged proteins were expressed as soluble proteins and subjected to an Amylose-resin affinity column (New England Biolabs), and eluted by raising the maltose concentration. This protein was coupled to N-hydroxysuccinimide-activated Sepharose (Amersham). Rat-liver cytosol was loaded onto the MBP-Mfn1ΔC column, and eluted by the indicated concentrations of NaCl.

cDNA cloning of rat MIB proteins

MIB was eluted from Coomassie Brilliant Blue-stained SDS-PAGE gel and subjected to tandem LC-Mass analysis after in-gel digestion. The protein sequence was found in the NCBI database (accession number NP_001028855). The following oligonucleotides were synthesized based on the deposited cDNA sequence. The 1215-bp fragment of rat MIB was amplified from rat liver poly(A)-RNA by RT-PCR using oligonucleotides as primers (MIB-N1, 5′-ATGTCGGCGGAG-AGGGAGGCA-3′; MIB-C1, 5′-CTAGGTCTCCTTCTCAGGCCCAGG-3′). The fragment was subcloned into the pTOPO II vector (Invitrogen).

Preparation of antibodies against rat MIB

The *Bam*HI-*Hin*dIII fragment (underlined) of rat MIB was amplified by PCR using rMIB cDNA as the template and the following primers: MIB-N2, 5′-ACG-GGATCCATGTCGGCGGAGAGGGAGGCA-3′; MIB-C2, 5′-CGTAAGCTTCT-AGGTCTCCTTCTCAGGCCC-3′. The obtained fragment was subcloned into the pET28a vector (Novagen). BL21 cells harboring the plasmid were cultured at 37°C in 1 mM IPTG for 5 hours. The supernatant fraction was incubated with TALON resin (Clontech). The resin was washed with 20 mM imidazole and His-tagged rMIB protein was eluted with imidazole (20-300 mM), and used to raise antibodies in rabbits. Specific IgG against MIB was selected using MIB-conjugated Formyl Cellulofine beads (Seikagaku Kogyo, Japan).

Construction of mammalian expression plasmids

The C-terminal flag-tagged MIB and C-terminal HA-tagged MIB proteins were constructed as follows. The PCR fragments of rat MIB were amplified by PCR using rMIB cDNA as the template using the following primers for MIB-FLAG (MIB-N-FLAG, 5′-ACTGGATCCCCACCATGTCGGCGGAGAGGGAGGCA-3′; MIB-C-FLAG, 5′-AGTGGATCCGGTCTCCTTCTCAGGCCCAGG-3′) and for MIB-HA (MIB-N-HA, 5′-ACTGAATTCCCACCATGTCGGCGGAGAGGGAGGCA-3′; MIB-C-HA, 5′-AGTTCTAGAGGTCTCCTTCTCAGGCCCAGG-3′). Underlined sequences denote the *Bam*HI restriction sites (for MIB-FLAG) and the *Eco*RI and *Xba*I (for MIB-HA). The obtained fragments were subcloned into *Bam*HI-digested p3xFLAG-CMV14 vector (Sigma) or *Eco*RI/*Xba*I-digested pcDNA3.1-HA vector (Ishihara et al., 2006).

Point mutations in or outside the CBD of the reductase domain were introduced by PCR with the primers having specifically mutated sequences (sequences will be provided on request). The mutated amino acid residues are shown in Fig. 4. All mutants were subcloned into *Eco*RI-*Xba*I-digested p3xFLAG-CMV14 vectors (Sigma).

hMIB-FLAG (Fig. 7A) was prepared as follows. The PCR fragment of hMIB was amplified by PCR using the human kidney cDNA library (Clontech) as the template and using *Eco*RI-site-containing primer and *Bam*HI-site-containing primer (sequences will be provided on request). The amplified fragments were subcloned into *Eco*RI-*Bam*HI digested p3xFLAG-CMV14 vector.

cDNA cloning of rat ζ-crystallin

The following oligonucleotides were synthesized based on the rat cDNA sequence of NCBI accession no. BC 078927. The 990-bp fragment of rat ζ-crystallin was amplified from rat liver poly(A)-RNA by RT-PCR using the following oligonucleotides as the primers: ζ-crystallin-N1, 5′-ACTAAGATCTCCACCAT-GGCAACTGGACAGAAGTTG-3′; ζ-crystalllin-C1, 5′-TAGTGGATCCTAAGA-GGAGAATCATTTTCCCCAT-3′. Underlined sequences denote the *Bgl*II and *Bam*HI restriction sites, respectively. The fragment was subcloned into the *Bgl*II-*Bam*HI-digested p3xFLAG-CMV14 vector.

Immunofluorescence microscopy

HeLa cells were cultured on coverslips in 35-mm dishes in 2 ml DMEM supplemented with 10% fetal bovine serum at 37°C overnight under an atmosphere of 5% CO_2. Transfection was performed using Lipofectamine (Lifetech). The cells were incubated for 24 hours and then stained with 20 nM of MitoTracker Red CMXRos (Molecular Probes) before fixation. The cells on the coverslips were fixed

Journal of Cell Science

with 4% paraformaldehyde for 30 minutes at room temperature, and then indirect immunofluorescence staining was performed as described previously (Ishihara and Mihara, 1998) using FITC-conjugated goat antibodies against rabbit IgG, Texas-Red-conjugated goat antibodies against rabbit IgG, FITC-conjugated goat antibodies against mouse IgG (BioSOURCE) or Cy5-conjugated goat antibodies against mouse IgG (Amersham/Pharmacia). Fluorescent images were analyzed using a confocal laser microscope Radiance 2000 (Bio-Rad).

Immunoprecipitation

HeLa cells expressing MIB-HA, Mfn1-FLAG, or Mfn2-FLAG, were lysed in lysis buffer (50 mM Tris-HCl buffer pH 7.5, containing 150 mM NaCl, 1 mM $MgCl_2$, 0.5 mM PMSF, 10 μg/ml α2-macroglobulin, protease inhibitor cocktail, and 1% digitonin) with or without 2 mM GTP. The lysates were cleared by centrifugation twice at 15,000 rpm for 5 minutes in a microcentrifuge, then the supernatant fractions were subjected to immunoprecipitation using polyclonal anti-HA antibodies and protein-A–Sepharose. The precipitates were analyzed by SDS-PAGE and subsequent immunoblotting using monoclonal anti-HA, anti-FLAG, or polyclonal anti-Tom40 antibodies.

RNA interference

For RNA interference (RNAi), 21-nucleotide small interference RNAs (siRNAs) comprising 19 nucleotides and a dTdT-overhang at each 3′-terminus were chemically synthesized (Elbashir et al., 2001). The synthesized siRNAs correspond to the 853-871 bp coding region in hMIB, regions that are not conserved between rats and humans (RNAi-MIB-1, 5′-AGAUACUGCCAAGGGCUACTT-3′; RNAi-MIB-2, 5′-GUAGCCCUUGGCAGUAUCUTT-3′).

siRNAs for GFP were purchased from B-bridge (Mountain View, CA). siRNAs for Mfn (Eura et al., 2003) and Fis1 (Jofuku et al., 2005) were described previously. HeLa cells grown in 35-mm dishes were transfected with the annealed siRNA duplex (2 μg) three times at 24-hour intervals using Oligofectoamine (Lifetech) and cultured for a further 24 hours.

Subcellular and submitochondrial fractionations

Subfractionation of rat liver cells was performed as described previously (Ishihara and Mihara, 1998). Sucrose-density-gradient centrifugation was performed as described by Mitoma and Ito (Mitoma and Ito, 1992). Briefly, the postnuclear supernatant was layered over a 2 M sucrose cushion, and centrifuged at 111,700 ***g*** for 1 hour to recover the postnuclear total membrane fraction. In a separate experiment, the postnuclear supernatant of rat liver homogenate was centrifuged at 2200 ***g*** for 10 minutes to precipitate the mitochondrial fraction, which was applied to density-gradient centrifugation as described above.

We thank members of Mihara laboratory for helpful discussion. This work was supported by grants from the Ministry of Education, Science, and Culture of Japan, from the Human Frontier Science Program, Core Research from Evolutional Science and Technology, and Takeda Science Foundation.

References

Alexander, C., Votruba, M., Pesch, U. E., Thiselton, D. L., Mayer, S., Moore, A., Rodriguez, M., Kellner, U., Leo-Kottler, B., Auburger, G. et al. (2000). OPA1, encoding a dynamin-related GTPase, is mutated in autosomal dominant optic atrophy linked to chromosome 3q28. *Nat. Genet.* **26**, 211-215.

Chan, D. C. (2006). Mitochondrial fusion and fission in mammals. *Annu. Rev. Cell Dev. Biol.* **22**, 79-99.

Chen, H. and Chan, D. (2004). Mitochondrial dynamics in mammals. *Curr. Top. Dev. Biol.* **59**, 119-144.

Chen, H., Detmer, S., Ewald, A., Griffin, E., Fraser, S. and Chan, D. (2003). Mitofusins Mfn1 and Mfn2 coordinately regulate mitochondrial fusion and are essential for embryonic development. *J. Cell Biol.* **160**, 189-200.

Cipolat, S., Martins de Brito, O., Dal Zilio, B. and Scorrano, L. (2004). OPA1 requires mitofusin 1 to promote mitochondrial fusion. *Proc. Natl. Acad. Sci. USA* **101**, 15927-15932.

Cuddenbach, S. M., Yamaguchi, H., Komatsu, K., Miyashita, T., Yamada, M., Singh, S. and Wang, H.-G. (2001). Molecular cloning and characterization of Bif-1: a novel Src momology 3 domain-containing protein that associates with Bax. *J. Biol. Chem.* **276**, 20559-20565.

Delettre, C., Lenaers, G., Griffoin, J. M., Gigarel, N., Lorenzo, C., Belenguer, P., Pelloquin, L., Grosgeorge, J., Turc-Carel, C., Perret, E. et al. (2000). Nuclear gene OPA1, encoding a mitochondrial dynamin-related protein, is mutated in dominant optic atrophy. *Nat. Genet.* **26**, 207-210.

Elbashir, S. M., Harborth, J., Lendeckel, W., Yalcin, A., Weber, K. and Tuschl, T. (2001). Duplexes of 21-nucleotide RNAs mediate RNA interference in cultured mammalian cells. *Nature* **411**, 494-498.

Escobar-Henriques, M., Westermann, B. and Langer, T. (2006). Regulation of mitochondrial fusion by the F-box protein Mdm30 involves proteasome-independent turnover of Fzo1. *J. Cell Biol.* **173**, 645-650.

Eura, Y., Ishihara, N., Yokota, S. and Mihara, K. (2003). Two mitofusin proteins, mammalian homologues of FZO, with distinct functions are both required for mitochondrial fusion. *J. Biochem.* **134**, 333-344.

Frank, S., Gaume, B., Bergmann-Leitner, E., Leitner, W., Robert, E., Catez, F., Smith, C. and Youle, R. (2001). The role of dynamin-related protein 1, a mediator of mitochondrial fission, in apoptosis. *Dev. Cell* **4**, 515-525.

Fritz, S., Weibach, N. and Westermann, B. (2003). Mdm30 is an F-box protein required for maintenance of fusion-competent mitochondria in yeast. *Mol. Biol. Cell* **14**, 2303-2313.

Hayess, K. H., Kraft, R., Sachsinger, J., Janke, J., Beckmann, G., Rohde, K., Jandrig, B. and Benndorf, R. (1998). Mammalian protein homologous to VAT-1 of *Torpedo californica*: isolation from Ehrlich ascites tumor cells, biochemical characterization, and organization of its gene. *J. Cell. Biochem.* **69**, 304-315.

Herlan, M., Vogel, F., Bornhovd, C., Neupert, W. and Reichert, A. S. (2003). Processing of Mgm1 by the rhomboid-type protease Pcp1 is required for maintenance of mitochondrial morphology and of mitochondrial DNA. *J. Biol. Chem.* **278**, 27781-27788.

Herlan, M., Bornhovd, C., Hell, K., Neupert, W. and Reichert, A. S. (2004). Alternative topogenesis of Mgm1 and mitochondrial morphology depend on ATP and a functional import motor. *J. Cell Biol.* **165**, 167-173.

Ishihara, N. and Mihara, K. (1998). Identification of the protein import components of the rat mitochondrial inner membrane, rTIM17, rTIM23, and rTIM44. *J. Biochem.* **123**, 722-732.

Ishihara, N., Eura, Y. and Mihara, K. (2005). Mitofusin 1 and 2 play distinct roles in mitochondrial fusion reactions via GTPase activity. *J. Cell Sci.* **117**, 6535-6546.

Ishihara, N., Fujita, Y., Oka, T. and Mihara, K. (2006). Regulation of mitochondrial morphology through proteolytic cleavage of OPA1. *EMBO J.* **25**, 2966-2977.

James, D. I., Parone, P. A., Mattenberger, Y. and Martinou, J. C. (2003). hFis1, a novel component of the mammalian mitochondrial fission machinery. *J. Biol. Chem.* **278**, 36373-36379.

Jofuku, A., Ishihara, N. and Mihara, K. (2005). Analysis of functional domains of rat mitochondrial Fis1, the mitochondrial fission-stimulating protein. *Biochem. Biophys. Res. Commun.* **333**, 650-659.

Karbowski, M. and Youle, R. J. (2003). Dynamics of mitochondrial morphology in healthy cells and during apoptosis. *Cell Death Differ.* **10**, 870-880.

Karbowski, M., Jeong, S.-Y. and Youle, R. (2004). Endophilin B1 is required for the maintenance of mitochondrial morphology. *J. Cell Biol.* **166**, 1027-1039.

Koch, A., Thiemann, M., Grabenbauer, M., Yoon, Y., McNiven, M. A. and Schrader, M. (2003a). Dynamin-like protein 1 is involved in peroxisomal fission. *J. Biol. Chem.* **278**, 8597-8605.

Koch, J., Foekens, J., Timmermans, M., Fink, W., Wirzbach, A., Kramer, M. D. and Schaefer, B. M. (2003b). Human VAT-1: a calcium-regulated activation marker of hyman epithelial cells. *Arch. Dermatol. Res.* **295**, 203-210.

Koshiba, T., Detmer, S. A., Kaiser, J. T., Chen, H., McCaffery, J. M. and Chan, D. C. (2004). Structural basis of mitochondrial tethering by mitofusin complexes. *Science* **305**, 858-862.

Lee, Y. J., Jeong, S. Y., Karbowski, M., Smith, C. L. and Youle, R. J. (2004). Roles of the mammalian mitochondrial fission and fusion mediators Fis1, Drp1, and Opa1 in apoptosis. *Mol. Biol. Cell* **15**, 5001-5011.

Linial, M. (1993). VAT-1 from Torpedo electric organ forms a high-molecular-mass protein complex within the synaptic vesicle membrane. *Eur. J. Biochem.* **216**, 189-197.

Linial, M. and Levius, O. (1993a). VAT-1 from Torpedo is a membranous homologue of zeta crystallin. *FEBS Lett.* **315**, 91-94.

Linial, M. and Levius, O. (1993b). The protein VAT-1 from Torpedo electric organ exhibits an ATPase activity. *Neurosci. Lett.* **152**, 155-157.

Linial, M., Miller, K. and Scheller, R. H. (1989). VAT-1: an abundant membrane protein from torpedo cholinergic synaptic vesicles. *Neuron* **2**, 1265-1273.

McQuibban, G. A., Saurya, S. and Freeman, M. (2003). Mitochondrial membrane remodelling regulated by a conserved rhomboid protease. *Nature* **423**, 537-541.

Messerschmitt, M., Jakobs, S., Vogel, F., Fritz, S., Dimmer, K. S., Neupert, W. and Westermann, B. (2003). The inner membrane protein Mdm33 controls mitochondrial morphology in yeast. *J. Cell Biol.* **160**, 553-564.

Mitoma, J. and Ito, A. (1992). The carboxy-terminal 10 amino acid residues of cytochrome b5 are necessary for its targeting to the endoplasmic reticulum. *EMBO J.* **11**, 4197-4203.

Mukamel, Z. and Kimchi, A. (2004). Death-associated protein 3 localizes to the mitochondria and is involved in the process of mitochondrial fragmentation durin cell death. *J. Biol. Chem.* **279**, 36732-36738.

Okamoto, F. and Shaw, J. (2005). Mitochondrial morphology and dynamics in yeast and multicellular eukaryoites. *Annu. Rev. Genet.* **39**, 503-636.

Olichon, A., Emorine, L. J., Descoins, E., Pelloquin, L., Brichese, L., Gas, N., Guillou, E., Delettre, C., Valette, A., Hamel, C. P. et al. (2002). The human dynamin-related protein OPA1 is anchored to the mitochhondrial inner membane facing the inter-membrane space. *FEBS Lett.* **523**, 171-176.

Olichon, A., Baricault, L., Gas, N., Guillou, E., Valette, A., Belenguer, P. and Lenaers, G. (2003). Loss of OPA1 perturbates the mitochondrial inner membrane structure and integrity, leading to cytochrome c release and apoptosis. *J. Biol. Chem.* **278**, 7743-7746.

Persson, B., Zigler, J. S., Jr and Jornvall, H. (1994). A super-family of medium-chain dehydrogenases/reductases (MDR). Sub-lines including zeta-crystallin, alchol and polyol dehydrogenases, quinone oxidoreductase, enoyl reductases, VAT-1 and other proteins. *Eur. J. Biochem.* **226**, 15-22.

Pierrat, B., Simonen, M., Cueto, M., Mestar, J., Ferrigno, P. and Heim, J. (2001). SH3GLB, a new endophilin-related protein family and SH3 domain. *Genomics* **71**, 222-234.

Sesaki, H. and Jensen, R. E. (1999). Division versus fusion: Dnm1p and Fzo1p antagonistically regulate mitochondrial shape. *J. Cell Biol.* **147**, 699-706.

Sesaki, H. and Jensen, R. E. (2004). Ugo1p links the Fzo1p and Mgm1p GTPases for mitochondrial fusion. *J. Biol. Chem.* **279**, 28298-28303.

Sesaki, H., Southard, S. M., Hobbs, A. E. and Jensen, R. E. (2003). Cells lacking Pcp1p/Ugo2p, a rhomboid-like protease required for Mgm1p processing, lose mtDNA and mitochondrial structure in a Dnm1p-dependent manner, but remain competent for mitochondrial fusion. *Biochem. Biophys. Res. Commun.* **308**, 276-283.

Shaw, J. M. and Nunnari, J. (2002). Mitochondrial dynamics and division in budding yeast. *Trends Cell Biol.* **12**, 178-184.

Suzuki, H., Okazawa, Y., Komiya, T., Saeki, K., Mekada, E., Kitada, S., Ito, A. and Mihara, K. (2000). Characterization of rat TOM40, a central component of the preprotein translocase of the mitochondrial outer membrane. *J. Biol. Chem.* **275**, 37930-37936.

Tondera, D., Santel, A., Schwarzer, R., Dames, S., Giese, K., Klippel, A. and Kaufmann, J. (2004). Knockdown of MTP18, a novel phosphadtidylinositol 3-kinase-dependent protein, affects mitochondrial morphology and induces apoptosis. *J. Biol. Chem.* **279**, 31544-31555.

Tondera, D., Czauderna, F., Paulick, K., Schwarzer, R., Kaufmann, J. and Santel, A. (2005). The mitochondrial protein MTP18 contributes to mitochondrial fission in mammalian cells. *J. Cell Sci.* **118**, 3049-3059.

Youle, R. J. and Karbowski, M. (2005). Mitochondrial fission in apoptosis. *Nat. Rev. Mol. Cell Biol.* **6**, 657-663.

Journal of Cell Science